# University of Cincinnati

**Date: 5/11/2012**

**I, Mounira A Habli M.D., hereby submit this original work as part of the requirements for the degree of Master of Science in Biostatistics (Environmental Health).**

It is entitled:

**Recapitulation of Human Placental Insufficiency in a Novel Mouse Model :New Paradigm in Translational Research**

Student's name: **Mounira A Habli M.D.**

This work and its defense approved by:

**Committee chair: Susan Pinney, PhD**

**Committee member: Timothy Crombleholme, MD**

UNIVERSITY OF Cincinnati

2594

# Recapitulation of Human Placental Insufficiency in a Novel Mouse Model: New Paradigm in Translational Research

A thesis submitted to the

Graduate School

of the University of Cincinnati

in partial fulfillment of the

Requirements for the degree of

Master of Science in Clinical and Translational Research

in the Department of Environmental Health

of the College of Medicine

Spring 2012

by

Mounira Habli, M.D.

Assistant Professor in Pediatrics Surgery Maternal Fetal Medicine

Cincinnati Children's Hospital Medical Center

Committee members: Susan Pinney (Chair)

Timothy Crombleholme M.D.

## Abstract

**Objective:** To develop a mouse model of placental insufficiency (PI) that recapitulates important characteristics of the human PI. We tested the effects of selective reduction of placental blood flow by mesenteric uterine artery branch ligation (MUAL) reliably resulting in fetal growth restriction (FGR).

**Methods:** At 18 days, timed mated C57BL/6J dams were divided into two groups: MUAL(n=18) ; and control-sham operated (n=18) with uterine horn fetal positions matched to each MUAL fetus. Pups were delivered on day 20, cross-fostered to surrogate CD-1 mothers for 4 weeks, and followed for 8 weeks. Outcome data included birth and placental weight, postnatal growth, placental volume determined by stereology, quantification of placental insulin-like growth factors-1(IGF-1) and IGF-2 and IGF binding proteins(IGFBP 2 and 6) by ELISA and gene expression by qPCR and GeneChip microarray analysis.

**RESULTS:** Compared with control, MUAL caused significant decrease (11%) in mean birth weight (1.06 ± 0.13 g vs. 0.94 ± 0.13 g, $p<0.001$) but no difference in placental weight (0.08 ± 0.03 g vs. 0.07 ±0.03 g,$p=0.6$). At 4 weeks of age, mean body weights of MUAL pups were also significantly lower than sham. By 8 weeks, males but not females MUAL mice achieved equivalent mean body weight to control. Placental labyrinth depth, volume, and placental gene expression of IGF-1 and 2 were significantly reduced by MUAL. In contrast, placental protein level of IGFBP-2 and 6 were significantly elevated in the MUAL. Genomic expression analysis profiling demonstrates that MUAL pups significantly up-regulated the expression of 344 genes, many of which were associated with apoptosis and growth-regulation related pathways.

**CONCLUSION:** This novel mouse animal model of FGR using selective mesenteric uterine artery ligation effectively recapitulates important characteristics of PI in humans. This is the first non-genetic mouse model of PI which offers its application in transgenic mice to better study the underlying mechanisms in PI.

ACKNOWLEDGEMENT

I would like to thank the members of thesis committee; Drs. Pinney and Cormbleholme for their guidance and support for developing this research. In particular, Dr. Crombleholme's suggestions have been invaluable for this project as well as my future goal toward an independent clinical research career.

I also would like to Helen Jones PhD, Department of Pediatric Surgery and Dr Bruce Aronow, PhD, Department of Bioinformatics, Cincinnati Children's Hospital for their support of this project.

TABLE OF CONTENTS

## Introduction

One of the most challenging complications in pregnancy is fetal growth restriction (FGR) for which there is no effective treatment.[1,2] This complication is the second leading cause of perinatal morbidity and mortality (exceeded only by prematurity),[3,4] with an incidence that ranges from 4 to 8% in developed countries and 6 to 30% of pregnancies in developing countries.[1,2] The most common cause of FGR, is placental insufficiency (PI), accounting for 75% of cases.[5,6] Affected infants suffer, not only from short-term[7,8] complications but long-term sequalae, such as hypertension and other diseases, in adult life.[9-11] There is an abundance of clinical and basic science studies that provide epidemiologic support for the phenomenological association between fetal growth restriction, and increased risk of adult diseases (i.e., obesity,diabetes, cardiovascular disease, cancer). [9-13] However, elucidation of the mechanisms that underlie this association or the biological mechanisms by which intrauterine growth restriction predisposes individuals to adult disease is incomplete. Lack of progress in this area is due mainly to the absence of a representative animal model of fetal growth restriction, which recapitulates the full spectrum of adult diseases later in life.

Several experimental models of FGR exits which use interventions, either in the mother (limitation of maternal carbohydrate and protein intake, uterine blood flow reduction) or in the fetus (genetic manipulation, infections, vascular interruption).[12-14] Most of the reported models are nutrition-based. Yet, human FGR is most commonly caused by placental insufficiency that occurs in the third trimester. One popular model of placental insufficiency is the Wigglesworth rat model,[15] which is induced by bilateral

uterine artery ligation. In a meta-analysis of rodent models of placental insufficiency, mostly the Wigglesworth rat model, Neitzke et al.[16] reported significant publication bias, specifically, inconsistent data regarding the prevalence and definition of fetal growth restriction at birth; they also noted a nonspecific distribution of birth weight in which the position of the fetus with lowest weight is near the uterine artery ligation site at the cervix and the position of the fetus with highest weight is near the ovarian end. Similarly, nutrition-induced FGR models produce a similar weight among all pups and inconsistent results regarding postnatal catch-up growth and development of adult diseases (e.g., metabolic syndrome, hypertension).[17-19] Considering the limitations and inconsistencies in these animal models, we sought a more appropriate, representative animal model would be a mouse model to study the pathophysiology and biologic mechanisms of FGR and possibly therapeutic intervention. Specifically, we wanted a reliable, reproducible mouse model with characteristics similar to human FGR for study of its pathophysiology in order to pursue a more complete understanding of the fetal and placental response to vascular insufficiency.

Human FGR is characterized by low circulating levels of insulin, IGF-I, and IGF-II, and high levels of IGFBP-1.[20,21] When pregnancy is complicated by fetal growth restriction, the placenta has specific morphologic characteristics, such decreased in total surface area, capillary surface area, trophoblast proliferation and volume of trophoblast component [22], and significant impairment of glucose and amino acid transporters.[23]

An ideal animal model of human placental insufficiency should recapitulate the changes in placental morphology, alterations in genomic expression profile, growth factor milieu, and transporter function. The mouse, with its proven usefulness in the study of many diseases, including the genetic basis of human disease, shares many anatomic similarities, including placental structure, with humans.[24,25] A surgical mouse model of placental insufficiency would be ideal by allowing its application in transgenic mice to study the pathogenesis, signaling pathways, transporter mechanisms, and possible treatments of PI.

**We hypothesized that selective ligation of a single mesenteric branch of the uterine artery (MUAL) to a specific gestational unit normally perfused by two MUAs will lead to fetal growth restriction (defined as <10$^{th}$ percentile for gestational age in a C57BL/6J mice) in that pup compared to position matched sham operated control. Our test specimens are compared with internal controls (same position in the opposite uterine horn) and external sham controls (matched by position). The effect of this model of placental insufficiency on birth weight and postnatal catch up growth, stereologic placental morphometric analysis, gene expression and protein levels of insulin-like growth factors (IGF)-1 and IGF-2 and their binding proteins (IGFBP-2 and IGFBP-6), as well as microarray gene expression profiling will be assessed.**

## Materials and Methods

### Mouse Model Development

The Institutional Animal Care and Use Committee of Cincinnati Children's Hospital Research Foundation approved this study. Time mated pregnant C57/BL6J mice were obtained from Charles River Laboratories (Wilmington, MA) housed under standard conditions and allowed free access to standard chow and water.

On day 18 of gestation (term 19-21 days), the dams underwent a laparotomy through a midline incision under continuous inhaled isoflurane anesthesia; mice included had 3 -6 pups in each uterine horn. The uterus was exteriorized and the gestational sacs of both horns were counted; each fetus was identified. Fetal position within the bicornuate uterus was defined as 1 for the fetus closest to the cervix and the last position at the ovarian end. Each fetus has its own segment of the uterus and its own placenta with its own blood supply. Each uteroplacental unit has either one or two uterine artery mesenteric branches. We included only fetuses whose placentas were supplied by two uterine artery mesenteric branches and then selective ligation of one branch using 4-0 silk was performed (Figure 1A). One fetus was ligated per pregnant mouse. The exteriorized uterus was continuously rinsed with warm Ringer's lactate solution to prevent desiccation. An abdominal cervical cerclage was performed to prevent premature delivery before surgical delivery on day 20 of gestation (Figure 1B). Fetuses at the ovarian end and the first fetal position were excluded from selection because of variation in uterine arterial perfusion. In each pregnant mouse, a specific fetal position who met our inclusion criteria was selected randomly for mesenteric uterine artery branch ligation in one uterine horn. This ligated fetus in one uterine horn

was then position matched to unligated fetus in the other uterine horn in the same pregnant mouse to serve as an internal control. In sham-operated dams (defined as a pregnant mouse exposed to the stress of surgery but with no ligation), fetuses matched to same position of the ligated fetus were used as external controls. The abdominal wall was closed by mass closure techniques using 2-0 vicryl.

On day 20 of gestation, a cesarean section was performed and the dams were delivered. After documenting the birth and placental weight of each fetus, the mothers were humanely killed. All placental specimens were either fixed or snap frozen for further analysis.

Primary outcome variable was the mean birth weight of ligated pups compared to internal controls and sham operated external controls. Fetal growth restriction was defined by birth weight at less than the$10^{th}$ percentile derived from sham operated fetal birth-weight distribution curves**.** This criterion is the same definition as the clinical definition of fetal growth restriction. Secondary outcome variables, including maternal survival after surgery and fetal survival until birth, were calculated by dividing the number of live fetuses at the time birth by the total number of viable fetuses at the end of surgery. At birth, we defined Group 1, Sham-operated external control with cerclage (n= 18 fetus); Group 2, Position-specific (MUAL) mesenteric uterine artery ligated group with cerclage (n= 18 fetus); and Group 3, Control as the matched position unligated fetus in the opposite uterine horn (n=18 fetus).

**Postnatal growth**

Postnatal growth trajectory pattern was evaluated in this novel mouse model. After birth weight validation of the model, in a new subset of mice, pups from both groups sham operated external controls (n=25) and mesenteric uterine artery-ligated group (n=32) were successfully resuscitated after cesarean delivery. Pups were cross fostered onto ad libitum-fed CD-1mice with a litter limited to 4 foster pups to normalize rearing. To reduce stress, pups were not handled during the first week of rearing. At 4 weeks of age, following weaning, offspring were individually housed and allowed food and water ad libitum. Weekly body weight was measured until 8 weeks of age. All animals were housed in a facility with constant temperature and humidity and a controlled 12:12 hour light/dark cycle.

**Immunohistochemistry**

Placental specimens from each group were fixed overnight at 4 °C in 10% paraformaldehyde immediately after dissection, embedded in paraffin, and cut into 5-um sections. Serial sections were deparaffinized in xylene and rehydrated, sections were incubated in Target Retrieval Solution (Dako, Carpathia, CA) at 95 degrees Celcius for 20 minutes. Sections were incubated for 10 min in 3% hydrogen peroxide to inhibit endogenous peroxidase. Nonspecific protein interactions were blocked using 5% Fish Skin Gelatin (Sigma, St. Louis, MO). Sections were then incubated with Meca-32 (Developmental Studies Hybridoma Bank, Iowa City, IA) and either Rabbit anti-Rat Alexa Fluor-647 conjugated secondary antibody (Invitrogen, Carlsbad, CA) or Rabbit anti-Rat IgG-HRP conjugated secondary antibody (Invitrogen). Slides were mounted with Prolong Gold Antifade Reagent plus DAPI (Invitrogen) or counterstained with

hematoxylin and mounted in Xylene mounting medium (Fisher, Kalamazoo. MI). For hematoxylin and eosin (H&E) standard staining protocol was followed.[26]

**Placental analyses**

**Gross structure**

Placentas from each group were collected and fixed in 4% paraformaldehyde for paraffin embedding following standard protocols. Special care was taken to place all the placentas in a standard orientation before embedding. Paraffin-embedded placentas were completely sectioned at 5 µm. Systematic random sampling throughout placenta was used to select sections for morphometric analysis. [27] All measurements were made independently by two investigators (MH, HJ) who were blinded to the groups. A Mean value of the two scores was used for statistical analysis.

**Stereologic Placental Morphometry**

**Volume measurements**

The proportion (volume density) of the placenta occupied by labyrinthine zone (Lz), was determined on a Nikon Eclipse 80i microscope (Nikon, Melville, NY) using the stereo investigator software ((MBF bioscience, Williston, VT). Absolute volumes were estimated using the Cavalieri principle estimator [28]. $V(obj)=t \times \Sigma a = t \times a(_p) \times \Sigma p$ where V(obj) is the estimated placental volume, t is the total thickness of the placenta (total number of sections 10 multiplied by section thickness 5µm), a (p) is the area associated with each point, and $\Sigma p$ is the sum of points on sections.

**Placental Labyrinth Depth**

Labyrinth depth as described by Dokras et al[29] was measured from H & E stained section on a Nikon Eclipse 80i microscope (Nikon, Melville, NY). The width of the labyrinth was determined by drawing a line parallel to its base, which identified the largest distance in the center of placenta from the lower margin of labyrinth above the chorionic plate to the transition point of the junctional zone (identified by morphological detection of trophoblast giant cells) using image analysis software (Image J, National Institutes of Health, Bethesda, MD) (Figure 3).

**Fetal Microvascular Identification and Analysis**

Fetal microvascular area determination in the labyrinth was performed at 40x magnification following immunohistochemical staining for Meca-32. Systematic random sampling was used as described above. Fetal microvascular area was measured using image analysis software (Image J, National Institutes of Health, Bethesda, MD) (Figure 4).

**RNA Isolation**

Total RNA was isolated from placentas using the RNEasy Mini kit (Qiagen) following the manufacturers standard protocol.

**Microarray hybridizations**

RNA integrity and quantification was done using an Agilent 2100 bioanalyser (Agilent, Santa Clara, CA). Triplicate sample sets for each treatment group (Sham external control and MUAL) were used to generate total RNA-based profiles using the

Affymetrix WT labeling kit(Affymetrix , Santa Clara, California) and Affymetrix GeneChip Mouse Genome 1.0 ST Arrays carried out by the Cincinnati Children's Affymetrix Microarray Core. Labeled cRNA synthesis, GeneChip hybridization, washing and staining followed standard Affymetrix protocols. The probed arrays were scanned with the Affymetrix GeneChip® Scanner 3000 7G and the intensities of array signals were captured with GeneChip Operating Software (GCOS) v1.1.0, according to standard Affymetrix procedures.

**Microarray Data Normalization and Analysis**

CEL files from the GCOS output were subjected to RMA(robust multichip average) normalization (Bolstad, Irizarry et al. 2003) using GeneSpring 7.1 (Agilent Technologies, Santa Clara, CA). Probe sets were filtered for those with RMA > 6.0 in either sample group average, and then for probe sets that differed significantly between the two groups by two-tailed Student's t-test ($p<0.05$). Variance was too high for False Discovery Rate (FDR) p-value adjustment. However, with use of strongly expressed genes and a threshold of >1.2X fold difference, a high proportion of tested mRNAs were confirmed by RT-PCR to be differentially regulated in separate samples.

**Functional classification of differentially expressed genes**

Significantly differentially expressed genes were subjected to an intensive search to identify biological functions using the ToppGene server.[30] The enriched functional categories were determined by Fisher Exact Test using the corresponding murine genome as a reference dataset. The significance was set at *p*-value < 0.05.

**Quantitative Real-Time PCR**

After RNA isolation, cDNA was synthesized using the High Capacity cDNA Reverse Transcription kit (Applied Biosystems, Foster City, CA) following suppliers instructions. SYBR green assays were designed to span intron/exon boundaries when possible. Oligonucleotides were aligned against the mouse genome by Primer-BLAST (www.NCBI.org) to ensure specificity. Gene expression was assayed, in triplicate in a Power SYBR Green PCR Master Mix reaction in the Applied Biosystems StepOne-Plus Real-Time PCR System (Applied Biosystems, Carlsbad, California). Gene expression was normalized to Beta-2-Microglobulin (B2M) gene expression. Relative expression values were calculated using the Comparative Ct (ΔΔCt) method (Pfaffl). Experiments were run in triplicate. Oligonucleotide primer sequences are listed in the supplemental information (Table I).

**Maternal serum and placental protein levels of insulin-like growth factor 1 and 2 and binding proteins 2 and 6**

Placental frozen tissues were powdered in a ceramic mortar with liquid nitrogen and, homogenized for 30 s with a mechanical homogenizer (Tissue Tearer, Biospec Inc. USA) in ice-cold Tissue Extraction Reagent 1 (Biosource International, Inc.,Camarillo, Calif., USA) supplemented with 1% Triton X-100 and anti-proteases (Complete, Mini, EDTA-free Protease Inhibitor Cocktail Tablets, Roche Applied Science, Basel, Switzerland) and centrifuged at 10,000 *g* for 5 min. The resulting supernatant was

collected and assayed for protein concentration using the BCA protein assay kit (Pierce, Rockford, Ill., USA) with bovine serum albumin (BSA) as a standard.

Maternal blood samples were collected at time of C-section day 20 from each experimental group and allowed to clot for 2 hours at room temperature or overnight at 2 - 8° C before centrifuging. Samples were centrifuged for 20 minutes at 2000 x g. Serum were removed and assayed immediately or aliquoted and stored at -20° C.

Maternal serum concentrations and placental protein levels of IGF-I were evaluated in triplicate using the commercial ELISA kit (cat # MG100, R&D Systems, Minneapolis,USA). The minimum detection limit was 3.5pg/ml. The intra- and inter-assay coefficients of variations (CVs) were 4.1 and <5%, respectively.

Maternal serum concentrations and placental protein levels of IGF-2 were evaluated in triplicate using the commercial ELISA kit (cat # DY792, R&D Systems, Minneapolis ,USA). The minimum detection limit was 9pg/ml. The intra- and inter-assay coefficients of variations (CVs) were both <10%.

Maternal serum concentrations and placental protein levels of IGFBP-2 were evaluated in triplicate using the commercial ELISA kit (cat# DY797, R&D Systems, Minneapolis ,USA). The minimum detection limit was 25pg/ml. The intra- and inter-assay coefficients of variations (CVs) were both <8%.

Maternal serum concentrations and placental protein levels of IGFBP-6 were evaluated in triplicate using the commercial ELISA kit (cat # ELM-IGFBP6-001, Ray Biotech, Georgia, USA). The minimum detection limit is 6 pg/ml. The intra- and inter-assay coefficients of variations (CVs) were <10 and <12%, respectively. Sample values

were normalized against total protein levels determined using BCA protein assay (Bio-Rad, California, USA).

**Statistical Analyses**

Statistical analyses were performed using SPSS 17.0.1 (SPSS Inc., Chicago, IL). Data were reported as mean ± standard deviation (SD) and frequencies as appropriate. Data were analyzed using student t-test, Fisher exact, and chi square as appropriate. Apriori estimation of sample size calculation for a study comparing two means was performed using the following equation for sample size (N, total number in both arms) = $4\sigma^2(Z\ critical(crit) + Z\ power(pwr))^2/D^2$ as described by Eng J et a.l[31] The σ is the assumed SD of each group (assumed to be equal for both groups), the *Z*crit and Zpwr, both are cutoff points along the x axis of a standard normal probability distribution that demarcate probabilities matching the specified significance criterion. *D* is the minimum expected difference between the two means. The sample size calculation was based on mean birth weight of pups at 20 days of gestation as 1.111±0.0856 gram, *Z*crit at p=0.05 =1.96, *Z* pwr at 80%=0.842,D=0.0997( 10% difference in weight). The minimum sample size in each arm is 12.

## Results

### Survival

There are no significant differences in overall maternal survival at birth: that is, 15 (83%) of the 18 sham dams group survived compared with 16 (89%) of the 18 specific MUAL group. Maternal deaths resulted from surgical complications that included wound dehiscence (n=2), infection (n=2), and bleeding (n=1).There are no significant differences in fetal mortality rate 19% (3/16 pups) in the MUAL group and 13% (2/15 pups) in the sham control group. Similarly, no significant differences are observed in postnatal survival to 8 weeks between the MUAL group 81% (27/32) and the sham control 92% (23/25) (p=0.42).

### Birth weight

To establish birth weight percentiles for C57/BL/6J at gestational age day 20, timed mated pregnant sham control mice (3-6 pups in each uterine horn, excluding first pup at cervical end and last pup at ovarian end) (n=4, 20 pups) delivered by C-section and were weighed at birth. Mean weight at birth was 1.111±0.0856 grams; the weights of 1.0118, 1.036, 1.257 g represent the $10^{th}$, $25^{th}$ and $90^{th}$ percentile, respectively. Distribution normality was tested using Shapiro-Wilk Test (sample size<50). The birth weight was normally distributed. No significant differences in fetal birth weight were observed between those with a single MUA branch compared with those who had more than one MUA branch supply matched by position (1.09±0.06 vs. 1.12± 0.095 gram, p=0.59). Sixty two percent (8/13=62%) had birth weight less than 10%(fetal growth restriction) in this model. Fetuses in the MUAL group (n=13) were significantly (p<0.001)

smaller at birth than sham external control (11% difference, $p<0.001$, n=13) and internal control groups (19% difference, n=13, $p<0.001$), respectively (Figure 2A). Placental weights did not significantly differ between the sham external control , internal control, and MUAL groups (0.08 ± 0.03 g vs. 0.07 ± 0.03 g vs. 0.07 ±0.03 g) ($p=0.6$), respectively.

**Postnatal Growth**

At 4 weeks of age, mice in the MUAL group (n=27) exhibited significantly lower bodyweights than those in the sham group (n=23, $p<0.001$) (Figure 2B). Data was stratified by sex to study the impact of sexual dimorphism during postnatal period. After weaning at 4 weeks and individual housing, only female MUAL mice (n=13) maintained significantly lower bodyweights compared with the female sham control group (n=9) (Figure 2C). However, male MUAL mice (n=14) mean bodyweight is equivalent to male sham control (n=14) mean bodyweight (data not shown).

**Placental structural analysis**

Both labyrinth depth (n>4 per group, $p<0.001$) and volume (n>4 per group, $p=0.014$) were significantly reduced after ligation compared with the sham controls (Figure 3B and C). The fetal micro-vascular area was also significantly diminished after ligation compared with sham controls ($p=0.002$, n>5 per group) (Figure 4D).

**Insulin-like Growth Factors and its Binding Proteins**

Significant reductions in placental expression of endogenous IGF-1, IGF-2 m RNA (Figure 5A and B) and placental protein levels of mouse IGF-1 (13.2±0.11 vs. 16.92 ±1.8 ng/mg total protein, p=0.03) in the MUAL group were observed in comparison with the sham control group. In contrast, no significant differences were found in placental protein levels of IGF-2 between MUAL and sham groups (99.89±7.26 vs.99.32±30 pg/ug protein, p>0.05) respectively. Placental protein levels of IGFBP-2 and 6 were significantly higher in the MUAL group compared with the sham control group (Figure 6).

Maternal serum protein levels of IGF-1, IGF-2 and IGFBP-2, however, did not significantly differ between sham and MUAL groups (data not shown). Interestingly, maternal serum protein levels of IGFBP-6 are significantly reduced in the MUAL group compared with the sham group (403.8±155 vs. 1092.7±173.3 ng/ml, p=0.001, n>4 per group).

**Placental Gene Expression Profile**

Global placental gene expression response to surgically-induced placental insufficiency was evaluated by the Affymetrix GeneChip Mouse Genome 1.0 ST oligonucleotide array. We compared expression levels between normal placentae at 20 days post-conception and those from pregnancies in MUAL. Of 28,853 well annotated genes represented by 770,317 distinct probes examined by the microarray, using the random variance model, we observed 408 transcripts were influenced by placental insufficiency ($p < 0.05$, F.C. > 1.4X). The vast majority of these (395 probes

corresponding to 344 known genes) were up-regulated (Table 2), and only 13 probe sets corresponding to 11 known genes were down-regulated (Table 3).

Functional cluster analysis of up-regulated genes revealed strong enrichment for genes associated with placental , spongiotrophoblast and labyrinth development (e.g., Prdx3, Ascl2, Dcn, Itgb8, Etnk2, Nsdhl,CITED1,DRG1), transforming growth factor B (TGFB) receptor activity, lipid metabolism,suppressors of cyotokine signaling,placental apoptosis(Caspase 6), solute channel genes (as Scl 35a5), genes coding for proteins with catalytic activity as(ADH1C,DLD) and epigenetic regulator (KDM6A)(Table 2). Representative genes with high signal intensity and relevance to growth were validated by real-time qPCR. Five placental genes are up regulated in MUAL vs. sham group : Caspase 6 (1.3 fold, apoptosis), CXCL14 (1.47 fold, inhibitor of trophoblast invasion), Ing-3(1.2 fold, tumor suppress gene that inhibit cell growth), SOCS6 (1.3fold, suppressor of cytokine signaling jak /STAT inhibitors) and Cathepsin F(CTSF)(1.25 fold, major component of the lysosomal proteolytic system). Two genes are down regulated genes ACTC 1(-0.7 fold, actin role and anti-angiogenic role,) and SLC7A10 (-0.8 fold, amnio acid transporter).

## Discussion

This is the first report of a surgically created murine model of fetal growth restriction due to placental insufficiency induced by mesenteric uterine artery branch ligation in a dual-supplied utero-placental unit at a specific uterine position. This novel mouse model is highly robust, reliable, reproducible and representative of human placental insufficiency with similar fetal and postnatal weight characteristics, placental morphology, and endocrine milieu to that of human fetal growth restriction with no significant impact on survival. The MUAL model, reliably results in a significant weight reduction that is less than the10$^{th}$ percentile for gestational age at birth analogous to the clinical definition of placental insufficiency. The MUAL model is also associated with postnatal catch up growth in the males but not the females through 8 weeks of age.

Previous studies have reported inconsistent postnatal growth trajectory of offspring after maternal bilateral uterine artery ligation. Although some authors demonstrated that FGR animals do not catch up in growth,[32-34] other groups have suggested that FGR animals do in fact catch up[35] or even surpass control animals in weight.[36] Sources of variability which may contribute to these inconsistencies include postnatal nutrition, control for sexual dimorphism, timing of uterine artery ligation (ranging from16 to 19 days gestation), and differences in animal strain. In our MUAL model of placental insufficiency, we found a significant difference between sham and the ligated group growth trajectories from birth to 8 weeks of age (Figure 2). After controlling for sexual dimorphism as of 4 weeks of age, male but not female MUAL mice regained sham-equivalent body weight. These findings are consistent with observations

in human and animal studies reporting the impact of sexual dimorphism on postnatal growth.[37]

Birth weight is known to be directly proportional to placental weight in normal gestation.[38]Several studies in human and FGR models in sheep and rat reported a significant decrease in total placental and capillary surface area and trophoblast volumes.[22,23] These findings are consistent with our findings of a significant decrease in labyrinth depth and volume and fetal microvascular area in the ligated group when compared with the sham group. These findings may be due to a reduction in cellular differentiation or proliferation and a concomitant increase in apoptosis based on the attenuation of placental gene expression profiles induced by MUAL. The observed up regulation of gene expression of apoptotic pathways[39] and cell growth inhibitors[40], as well as down regulation of angiogenic pathways[41] in this MUAL group, have been reported and are consistent with data in other animal models of FGR and in humans.

Placental morphologic derangement during development can adversely impact feto – maternal transport of gases, nutrients, and metabolites with resulting abnormal hormonal production of IGF-1 and 2. The IGF signaling system is known to play a critical role in normal physiologic growth of the fetus and placenta and shows alterations in various disease states (e.g., fetal growth restriction, diabetes), both in the fetus and postnatally.[42,43] The bioavailability of IGF-1 and 2 is inversely related to circulating levels of IGFBP-1 to 6.[44] Several reports show an inverse relationship between birth weight and the activity of the fetal IGF system (IGF-1 and 2)[42]; other studies also show a linear

direct relationship between birth weight and placental and fetal plasma levels of IGFBPs respectively.[44] These observations are consistent with our findings of decrease in placental m RNA expression of endogenous IGF-1, IGF-2 and increase in protein levels of IGFBP-2 , IGFBP-6 in IUGR animals as compared to sham control.

The molecular machinery underlying placental development and function in placental insufficiency is complex. DNA microarray analysis is a powerful tool to survey differential expression of gene products and has provided valuable information about the networks of molecular signals that regulate the biology and pathology of placenta in normal and pathological conditions. In our study, interestingly, 7 of the down-regulated genes were host genes for microRNAs or noncoding RNAs (MicroRNA 23a, 27a, 341, 342, let 7i, 125a, 99b) and targets for these microRNAs were strongly overrepresented in the up-regulated gene list as caspase 6 and SMAD gene family (Supplement 1). Recently, several reports showed that MicroRNA 23a, 125a, 27a reduction is associated with apoptosis involving P-53 and tumor necrosis factor α (TNF α) pathways[45-46]. In this model, up-regulation of caspase6, an effector target in TNF α pathway signaling pathway and the activation of other apoptotic genes (Table II) suggests that induction of apoptosis contributes to placental insufficiency pathophysiology in this murine model and this may be regulated by MicroRNAs as microRNA 125a[45]. Further, reduction in MicroRNA let7i has been shown in-vitro to increase branching points of mouse brain endothelial cells possibly by up-regulation of SMAD genes[47] suggesting a potential role of MicroRNAs in the microvasuclar changes in this murine model. We also found that most of the predicted up-regulated genes are associated with pathways involved in placental development, body weight and other pathways as transforming growth factor β

a potent multifunctional cytokine contributing to stromal epithelial interactions(Table II). These novel findings especially the microRNAs and their role in placental development and fetal growth warrant further investigations.

There is significant experimental appeal in this MUAL model because mice are in expensive, small and easily-manipulated animals with a short generation time. Compared with other rodents, a major benefit of mice is the availability of embryonic stem cells, which facilitates gene targeting for the development of transgenic mice. Our MUAL model has the advantage of using a specific uterine position that eliminates position bias. Further, mesenteric uterine artery branch ligation to induce FGR is more reliable, reproducible, and better recapitulates placental insufficiency in humans. The pups birth weight in this MUAL model meet the clinical definition of fetal growth restriction less than $10^{th}$ percentile similar to human data of FGR. In contrast, in the Wigglesworth model of bilateral uterine artery ligation, FGR is not well defined. Rather any pup whose weight is less than control is considered FGR. One of the major limitations of working in mice is that all rodents are altricial animals born with an underdeveloped brain and endocrine /paracrine system with significant organ maturation occurring during the weaning period. Despite this developmental feature of mice, short-term outcomes at birth and disease pathogenesis of this MUAL model of FGR offers a superior alternative to previously reported animal models of FGR.

## Conclusions

This MUAL is a new model of placental insufficiency which recapitulates clinical human data. The MUAL model may offer a new paradigm for the study of mechanisms of FGR by the application of the MUAL technique in placental specific conditional knockout mice aiding in the understanding of the pathophysiology of fetal growth restriction and the development of novel therapeutic strategies.

**References**

1. Niebyl JR, Simpson JL, Gabbe SG. Chapter 29: Intrauterine growth restriction. In: Baschat A, Galan H, Ross M, Gabbe SG, et al., eds. Obstetrics: Normal and Problem Pregnancies. 5th ed. New York: Churchill Livingstone, 2007:771-815

2. Wolfe HM, Gross TL. Increased risk to the growth retarded fetus. In: Gross TL, Sokol RJ, eds. Intrauterine Growth Retardation: A Practical Approach. Chicago: Year Book Medical Publishers, 1989:111-24.

3. Battaglia FC, Lubchenco LO. A practical classification of newborn infants by weight and gestational age. J Pediatr 1967;71:159-163 .

4. Jahn A, Razum O, Berle P. Routine screening for intrauterine growth retardation in Germany: low sensitivity and questionable benefit for diagnosed cases. Acta Obstet Gynecol Scand 1998;77:643-648.

5. Creasy RK, Resnik R. Chapter 34:Intrauterine growth restriction. In: Creasy RK, Resnik R, eds. Maternal-fetal Medicine: Principles and Practice. 6th ed. Philadelphia: Saunders, 2008:635-650.

6. Neerhof MG. Causes of intrauterine growth restriction. Clin Perinatol 1995;22:375-85.

7. Jones RA, Robertson NR. Problems of the small-for-dates baby. Clin Obstet Gynaecol 1984;11:499-524.

8. Alkalay AL, Graham JM Jr, Pomerance JJ. Evaluation of neonates born with intrauterine growth retardation: review and practice guidelines. J Perinatol 1998;18:142-151

9. Barker DJ, Hales CN, Fall CH, Osmond C, Phipps K, Clark PM. Type 2 (non-insulin-dependent) diabetes mellitus, hypertension and hyperlipidaemia (syndrome X): relation to reduced fetal growth. Diabetologia 1993;36:62--67

10. Eriksson JG, Forsen T, Tuomilehto J, Winter PD, Osmond C, Barker DJ. Catch-up growth in childhood and death from coronary heart disease: longitudinal study. BMJ 1999; 318:427—431.

11. Barker DJP. Intrauterine programming of coronary heart disease and stroke .Acta Paediatr. 1997; Suppl 423:178–182.

12.Ozanne SE. Metabolic programming in animals. Br Med Bull 2001; 60:143–152.

13.Vuguin P. Animals models for assessing the consequences of intrauterine growth retardation on subsequent glucose metabolism of\ the offspring: a review. J Matern Fetal Neonatal Med 2002; 254–257.

14.Petry CJ, Ozanne SE, Hales CN. Programming of intermediary metabolism. Mol Cell Endocrinol 2001;185: 81–91

15. Wigglesworth JS. Experimental growth retardation in the foetal rat. J Pathol Bacteriol 1964; 88:1-13.

16. Neitzke U, Harder T, Schellong K, Melchior K, Ziska T, Rodekamp E, Dudenhausen JW, Plagemann A. Intrauterine growth restriction in a rodent model and developmental programming of the metabolic syndrome: a critical appraisal of the experimental evidence. Placenta 2008 29(3):246-254.

17.Garofano A, Czernichow P. Bre´ ant B.Effect of ageing on beta-cell mass and function in rats malnourished during theperinatal period. Diabetologia 1999; 42:711–718.

18. Ozanne SE, Wang CL, Dorling MW, PetryCJ. Dissection of the metabolic actions of insulin in adipocytes from early growth retarded male rats. J Endocrinol 1999;162:313–319.

19. Petry CJ, Ozanne SE, Wang CL, Hales CN. Early protein restriction and obesity independently induce hypertension in 1-year old rats. Clin Sci 1997;93:147–152.

20. de Zegher F , Francois I , van Helvoirt M , Van den Berghe G. Small as fetus and short as child: from endogenous to exogenous growth hormone . J Clin Endocrinol Metab 1997; 82: 2021–2026.

21. Giudice LC, de Zegher F, Gargosky SE, Dsupin BA, de las Fuentes L, Crystal RA, Hintz RL, Rosenfeld RG . Insulin-like growth factors and their binding proteins in the term and preterm human fetus and neonate with normal and extremes of intrauterine growth . J Clin Endocrinol Metab 1995;80:1548–1555.

22. Mayhew TM. A stereological perspective on placental morphology in normal and complicated pregnancies. J Anat 2009;215:77–90.

23. Belkacemi L, Nelson DM, Desai M, Ross MG. Maternal undernutrition influences placental-fetal development. Biol Reprod 2010;83(3):325-331.

24. Cross JC, Hemberger M, Lu Y, Nozaki T, Whiteley K, Masutani M, Adamson SL. Trophoblast functions, angiogenesis and remodeling of the maternal vasculature in the placenta. Mol Cell Endocrinol 2002;187(1-2):207-212.

25. Georgiades P, Ferguson-Smith AC, Burton GJ. Comparative developmental anatomy of the murine and human definitive placenta. Placenta 2002;23(1):3-19.

26. Drury RAB, Wallington EA. Carlton's Histological Technique, 5th ed. Oxford: Oxford University Press; 1980:138–144.

27. Gundersen HJG, Jensen EB. The efficiency of systematic sampling in stereology and its prediction. J Microsc 1987;147:229–262.

28. Coan PM, Ferguson-Smith AC, Burton GJ. Developmental dynamics of the definitive mouse placenta assessed by stereology. Biol Reprod 2004;70(6):1806-1813.

**29.** Dokras A, Hoffmann DS, Eastvold JS, Kienzle MF, Gruman LM, Kirby PA, Weiss RM, Davisson RL. Severe feto-placental abnormalities precede the onset of hypertension and proteinuria in a mouse model of preeclampsia. Biol Reprod. 2006 Dec;75(6):899-907.

30. Chen J, Bardes EE, Aronow BJ, Jegga AG. ToppGene Suite for gene list enrichment analysis and candidate gene prioritization. Nucleic Acids Res 2009;37:305-311

31. Eng J. Sample size estimation: how many individuals should be studied? Radiology 2003; 227(2):309-313.

32.Houdijk EC, Engelbregt MJT, Popp-Snijders C, Delemarre-Vd Waal HA. Endocrine regulation and extended follow up of longitudinal growth in intrauterine growth-retarded rats. J Endocrinol 2000;166:599-608.

33. Huizinga CT, Engelbregt MJT, Rekers-Mombarg LTM, Vaessen SFC, Delemarre-van de Waal HA, Fodor M. Ligation of the uterine artery and early postnatal food restriction –animal models for growth retardation. Horm Res 2004;62:233-240.

34.Jansson T and Lambert GW. Effect of intrauterine growth restriction on blood pressure, glucose tolerance and sympathetic nervous system activity in the rat at 3-4 months of age. J Hypertension 1999;17:1239-1248.

35. Styrud J, Eriksson UJ, Grill V, Swenne I. Experimental intrauterine growth retardation in the rat causes a reduction of pancreatic B-cell mass, which persists into adulthood. Biol Neonate 2005; 88:122-128.

36. Simmons RA, Templeton LJ, Gertz SJ. Intrauterine growth retardation leads to the development of type 2 diabetes in the rat. Diabetes 2001; 50: 2279-86.

37. Claris O, Beltrand J, Levy-Marchal C. Consequences of intrauterine growth and early neonatal catch-up growth. Semin Perinatol 2010;34(3):207-210.

38. Salafia CM, Zhang J, Charles AK, Bresnahan M, Shrout P, Sun W, Maas EM. Placental characteristics and birthweight. Paediatr Perinat Epidemiol 2008;22:229-239.

39. Sharp AN, Heazell AE, Crocker IP, Mor G. Placental apoptosis in health and disease. Am J Reprod Immunol 2010;64(3):159-169.

40. Kuang H, Chen Q, Zhang Y, Zhang L, Peng H, Ning L, Cao Y, Duan E. The cytokine gene CXCL14 restricts human trophoblast cell invasion by suppressing gelatinase activity. Endocrinology 2009;150(12):5596-5605.

41. Barut F, Barut A, Gun BD, Ozdamar SO, et al . Intrauterine growth restriction and placental angiogenesis. Diagn Pathol 2010;22;5:24-31

42. Randhawa R , Cohen P. The role of the insulin-like growth factor system in prenatal growth. Mol Genet Metab 2005;86:84–90

43. Cetin I, Foidart JM, Miozzo M, Raun T, Jansson T, Tsatsaris V, Reik W, Cross J, Huppertz B et al. Fetal growth restriction: a workshop report. Placenta 2004; 25:753–757

44. Christians JK, Gruslin A. Altered levels of insulin-like growth factor binding protein proteases in preeclampsia and intrauterine growth restriction. Prenat Diagn 2010; 30(9):815-820.

45. Zhang Y, Gao JS, Tang X, et al. MicroRNA 125a and its regulation of the p53 tumor suppressor gene. FEBS Lett. 2009 Nov 19;583(22):3725-30.

46. Ruan W, Xu JM, Li SB, Yuan LQ, Dai RP.Effects of down-regulation of microRNA-23a on TNF-a-induced endothelial cell apoptosis through caspase-dependent pathways. Cardiovasc Res. 2012 Mar 15;93(4):623-32

47. Roitbak T, Bragina O, Padilla JL, Pickett GG. The role of microRNAs in neural stem cell-supported endothelial morphogenesis. Vasc Cell. 2011 Nov 9;3:25.

**Figure Legends**

**Figure 1: A)** Photograph of an exteriorized mouse uterus highlighting the site of ligation on one of two branches of the uterine artery supplying the identified placenta. **B)** Representative photograph demonstrating the site of abdominal cerclage using 2-0vicryl suture.

**Figure 2: A)** Offspring birth weight following ligation (MUAL, n=18) is significantly reduced compared to both sham-operated (n=18) and internal control animals(IC, n=18) at day 20. **B)** During the fostering period offspring weight remains significantly lower in ligated animals (FGR, n=32) than sham (n=25). **C)** Summary data for female offspring aged 5-8 weeks following ligation or sham surgery. (*p=0.03, *** p=0.001).

**Figure 3: A)** Representative photomicrograph (20x magnification) of a mouse placenta. Labyrinth depth measured by a perpendicular line from edege of junctional zone to the edge of the labyrinth distinguished from chorioallantois layer. **B)** Summary of placental labyrinth depth in Sham and Ligated animals(***p=0.005) **C)** Labyrinth volume is significantly reduced in placentas following ligation at gestational day 20(*p=0.014).

**Figure 4:** Representative photomicrographs of placental labyrinth following anti-Meca-32 immunohistochemistry in sham **(A)** and ligated **(B).(C)** 40x magnification for identification of fetal vessels (FV), fetal endothelial cells stain positive (brown) for Meca-32, syncytiotrophoblast (SCT) and maternal blood sinuses (MBS) Gross evidence of decrease in fetal vessel count in ligated as compared to Sham. **(D)** Summary data of fetal vessel area as identified by Meca-32 staining(***p=0.002)

**Figure 5:** Summary data for IGF-1 **(A)**(*p=0.01) and IGF-2 **(B)** (*p=0.03) RNA expression in total placenta from Sham or Ligated(UABL) animals normalized to Beta-2 Microglobulin expression.

**Figure 6:** Summary data for protein expression of IGFBP-2 and IGFBP-6 as determined by ELISA.

**Figure 1**

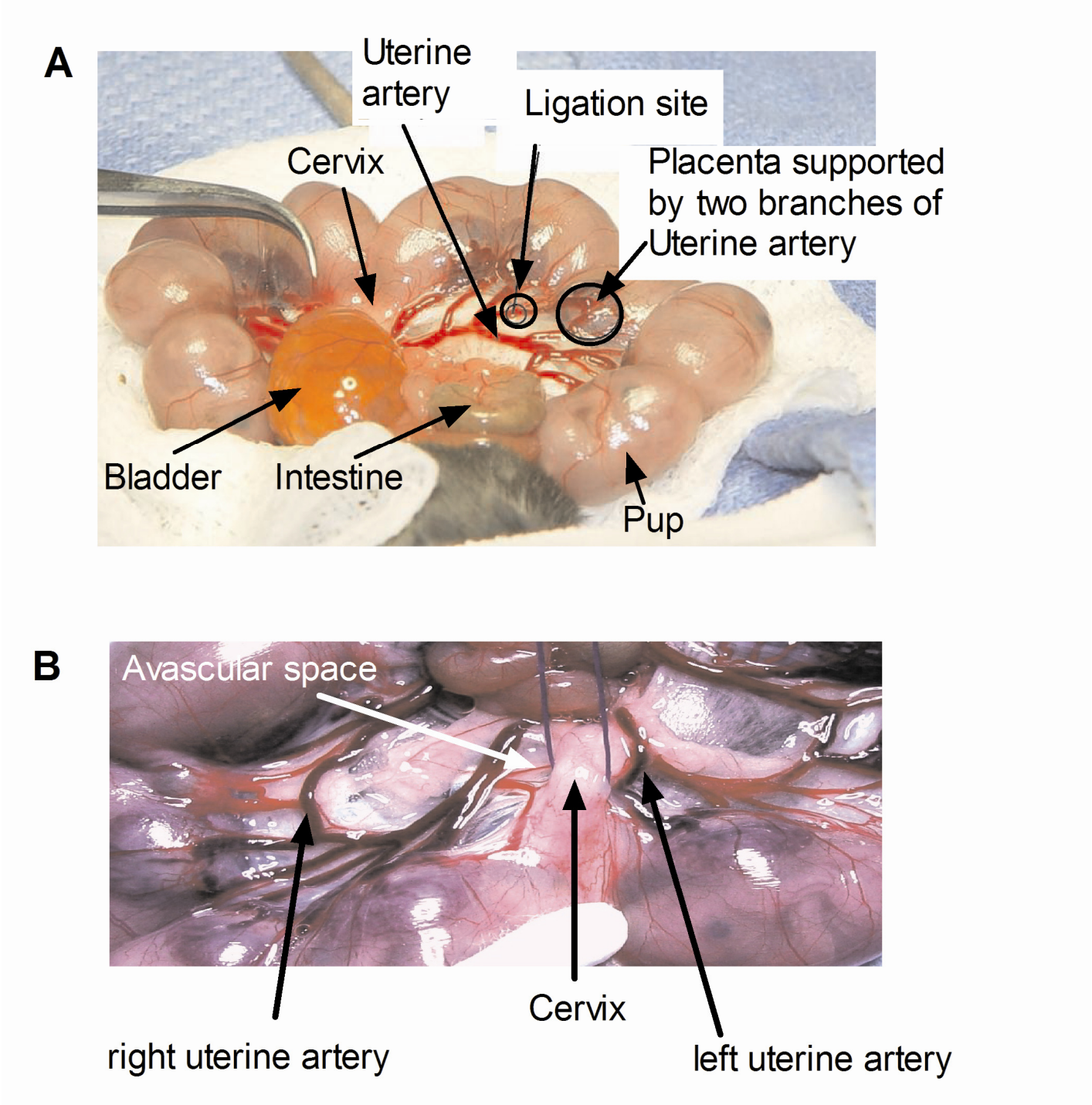
A
Uterine artery
Ligation site
Cervix
Placenta supported by two branches of Uterine artery
Bladder
Intestine
Pup
B
Avascular space
Cervix
right uterine artery
left uterine artery

**Figure 2**

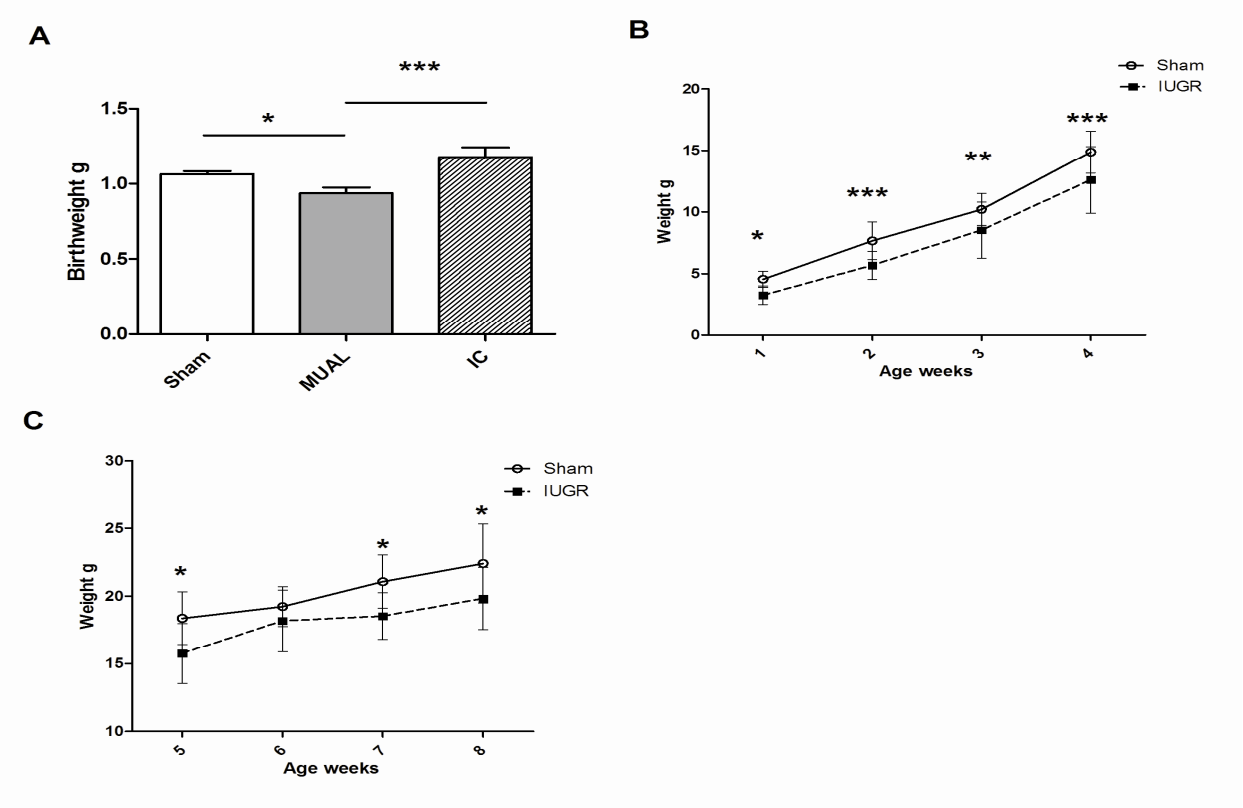


**Figure 3**

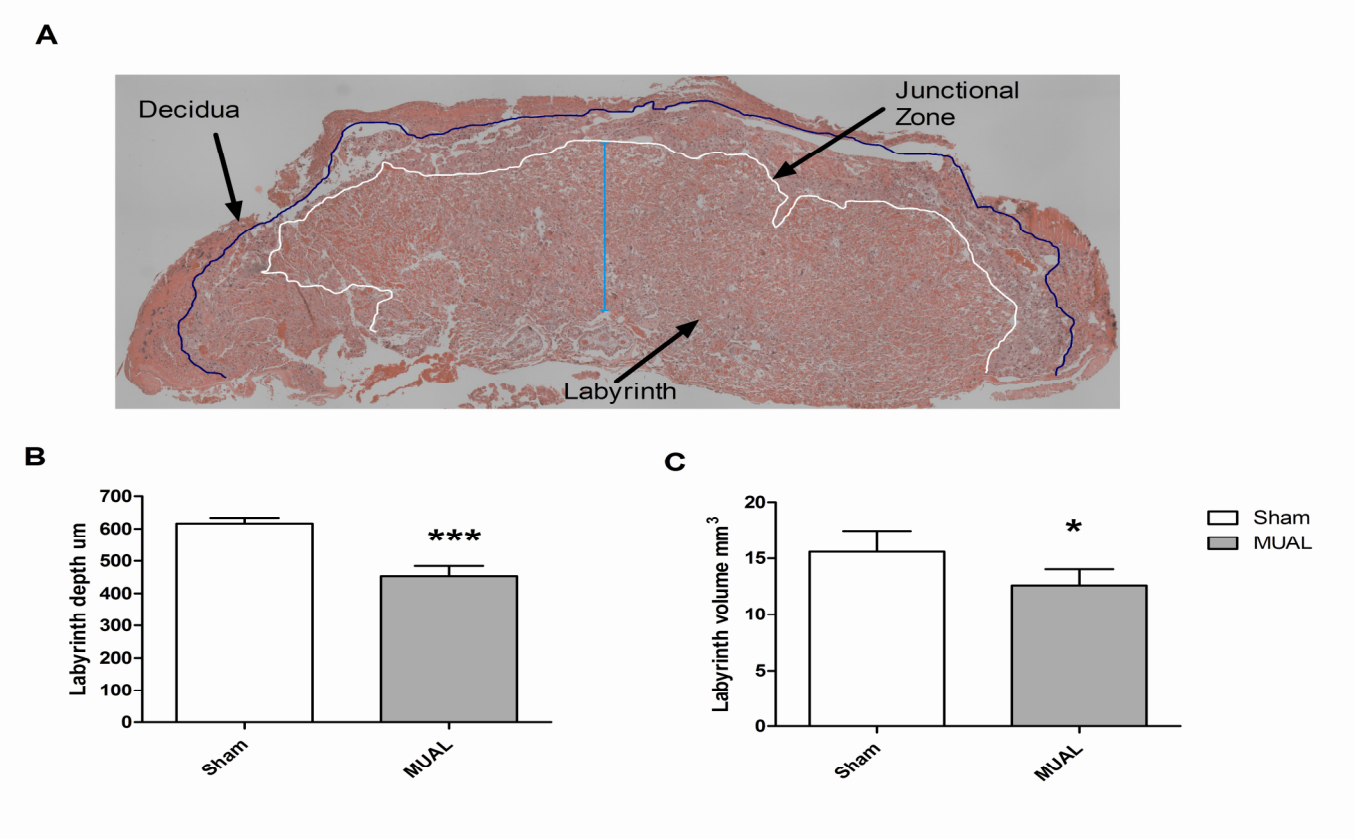
A
Decidua
Junctional Zone
Labyrinth
B
Labyrinth depth um
700
600
500
400
300
200
100
0
***
Sham
MUAL
C
Labyrinth volume mm3
20
15
10
5
0
*
Sham
MUAL
Sham
MUAL

**Figure 4**

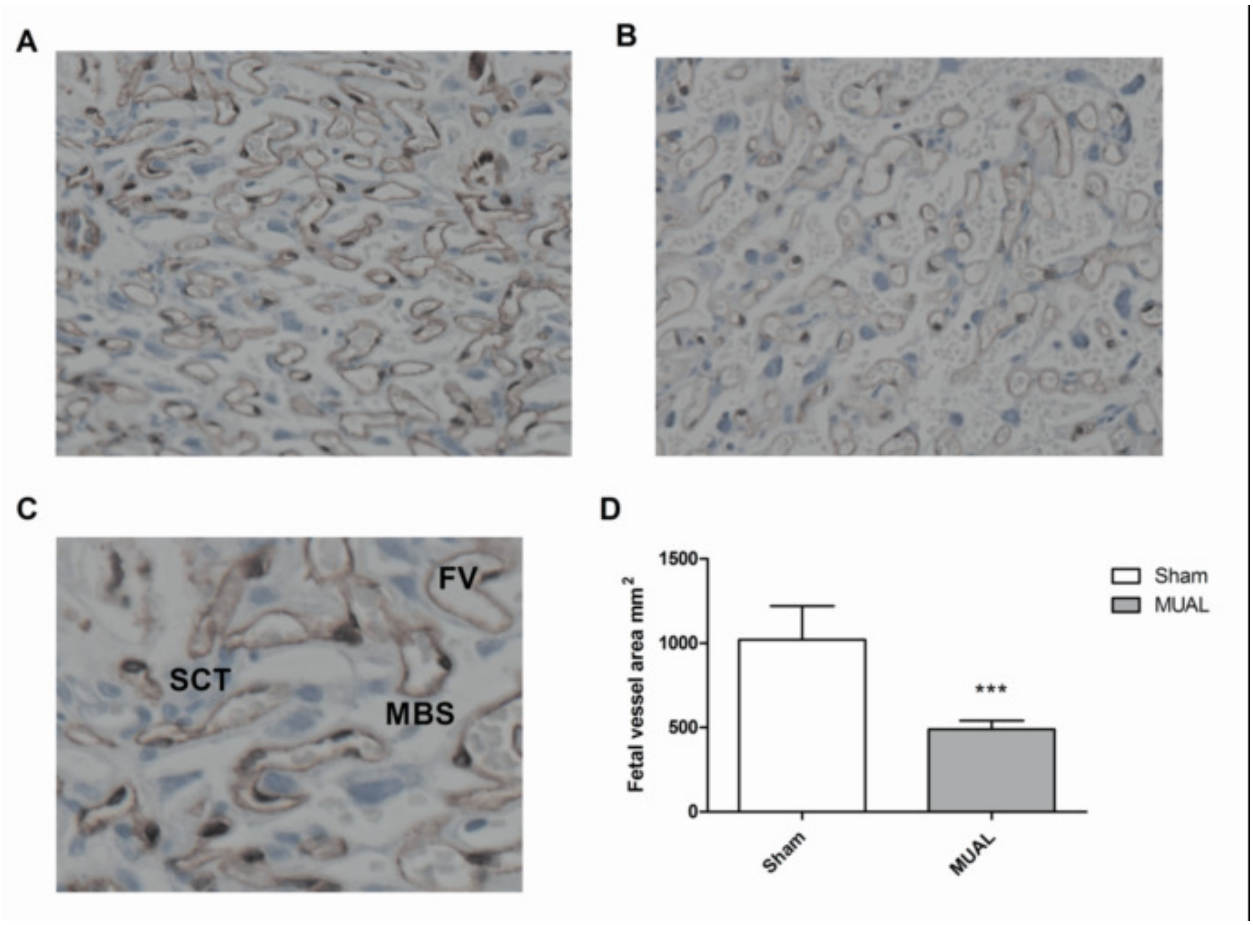
A
B
C
FV
SCT
MBS
D
Fetal vessel area mm²
1500
1000
500
0
***
Sham
MUAL
Sham
MUAL

**Figure 5**

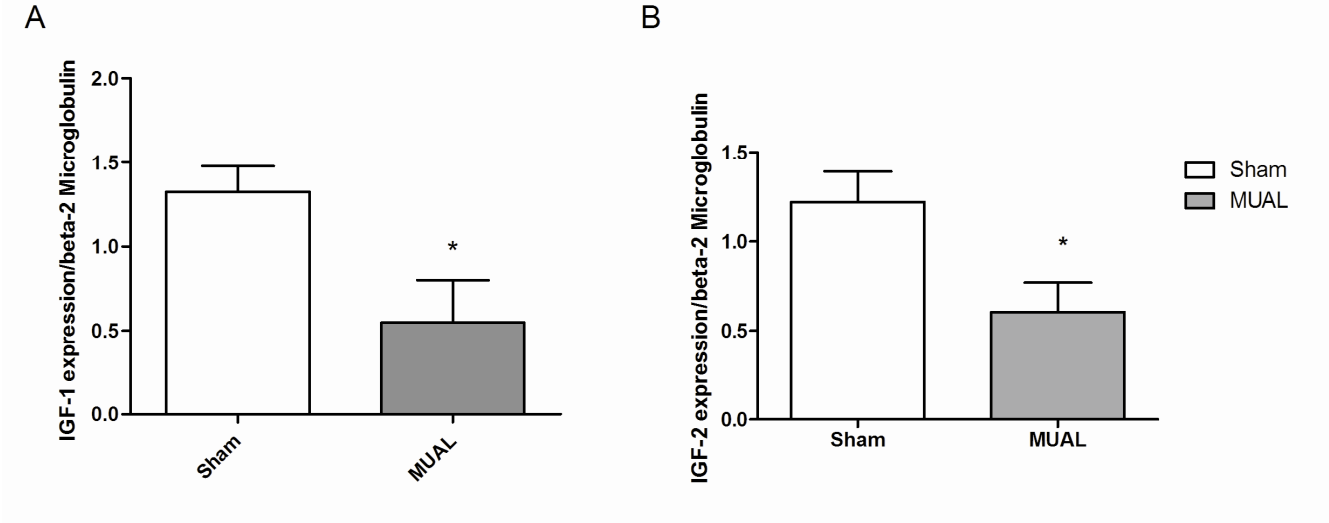
A
IGF-1 expression/beta-2 Microglobulin
2.0
1.5
1.0
0.5
0.0
*
Sham
MUAL
B
IGF-2 expression/beta-2 Microglobulin
1.5
1.0
0.5
0.0
*
Sham
MUAL
Sham
MUAL

**Figure 6**

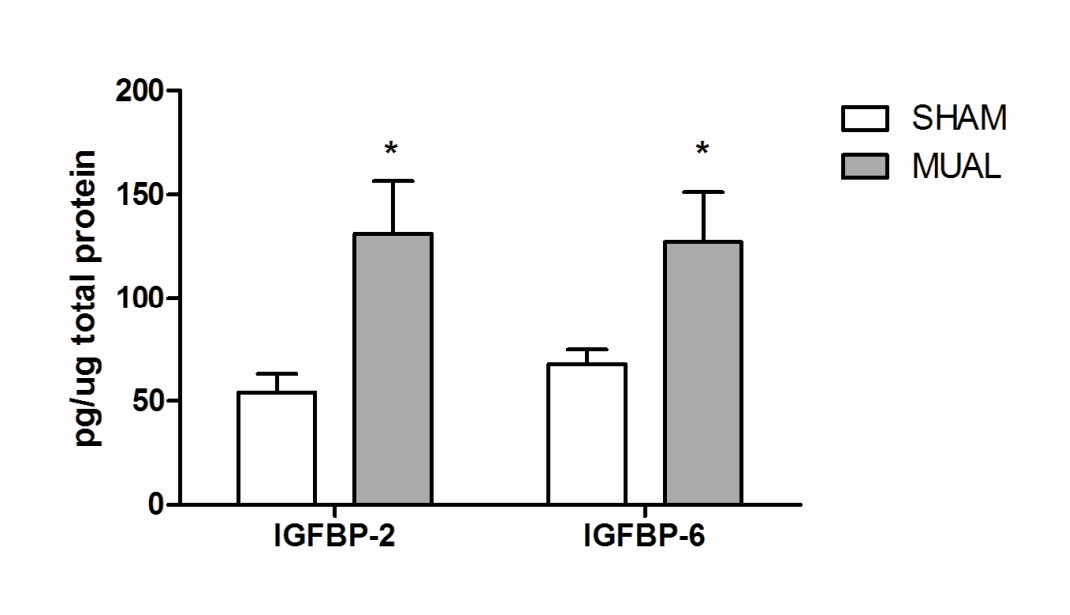

**Table 1:** Oligonucleotide primer sequences for qPCR validation of Microarray and Insulin-like Growth Factors-1 (IGF-1) and IGF-2 .

| Oligo Name | Gene Name | 5' to 3' Sequence | Amplicon Size (bp) | Intron Spanning |
|---|---|---|---|---|
| Mo Actc1 1F | Actin 1 | GCT GTC TTC CCG TCC ATC | 93 | Yes |
| Mo Actc1 1R | Actin 1 | CTG GGC TTC ATC ACC TAC AT | | |
| Mo B2M 1F | Beta-2-Microglobulin | TGC TAT CCA GAA AAC CCC TC | 102 | Yes |
| Mo B2M 1R | Beta-2-Microglobulin | AGG CGG GTG GAA CTG TG | | |
| Mo Casp6 1F | Caspase 6 | GCA GAA GAA CTC CTG CTC AA | 85 | Yes |
| Mo Casp6 1R | Caspase 6 | GGC TCA GGA AGA CAC AGA TG | | |
| Mo Cstf 2F | Cathepsin F | AAC GCC TAT GCA GCC ATA AA | 85 | Yes |
| Mo Cstf 2R | Cathepsin F | AGT TGC AGG TCT GAA CAT GG | | |
| Mo CXCL14 2F | Chemokine ligand 14 | GCT GCT CCT GCT GCT CCT | 94 | Yes |
| Mo CXCL14 2R | Chemokine ligand 14 | CGT CGC TGT AGC GGA TCT TG | | |
| Mo Ing3 1F | Inhibitor growth family member 3 | GCC ATC ACA CAG GCA GAT AA | 75 | No |
| Mo Ing3 1R | Inhibitor growth family member 3 | CGC GTT CTC TCG ATT CTC AT | | |
| Mo Slc7a10 1F | Solute carrier family 7 (cationic amino acid transporter, y+ system) | GGT GGC ACT CAA GAA AGA GA | 75 | Yes |
| Mo Slc7a10 1R | Solute carrier family 7 (cationic amino acid transporter, y+ system) | ATG CCT GAG CCA ATG ATG TT | | |
| Mo Socs6 1F | Suppressor of cytokine signaling 6 | TGC CTC CAT AAG ATT TGC CT | 78 | Yes |
| Mo Socs6 1R | Suppressor of cytokine signaling 6 | CGA TGC CTC ATG GGT GTA TT | | |
| MO Igf1 1F | Insulin like Growth Factor-1 | TGG ATG CTC TTC AGT TCG TG | 101 | Yes |
| MO Igf1 1R | Insulin like Growth Factor-1 | CAC AAT GCC TGT CTG AGG TG | | |
| MO Igf2 1F | Insulin like Growth Factor 2 | CGC TTC AGT TTG TCT GTT CG | 97 | Yes |
| MO Igf2 1R | Insulin like Growth Factor -2 | AAG CAG CAC TCT TCC ACG AT | | |

Table II: Summary of up-regulated placental genes in Novel Mouse Model of Placental insufficiency.

| Category | Phenotype | Gene name | P-value |
|---|---|---|---|
| BP | Placental development | PRDX3,CITED1,ADM,ASCL2,DCN,ITGB8,ETNK2, NSDHL,SP1 | 0.00013 |
| BP | Spongiotrophoblast layer development | CITED1,ADM,ASCL2 | 0.00046 |
| BP | Embryonic placenta development | CITED1,ADM,ASCL2,NSDHL,SP1 | 0.00797 |
| BP | Labyrinthine layer development | CITED1,ADM,NSDHL | 0.02951 |
| BP | Cellular response to hypoxia | VLDLR,AQP1 | 0.01095 |
| BP | Regulation of transforming growth factor beta receptor signaling pathway | CITED1,SMAD6,SMAD7,NPNT | 0.03386 |
| BP | Positive regulation of TOR signaling | GOLPH3,RHEB | 0.02262 |
| BP | Branched amino acid catabolic process | ACADSB,HIBADH,AUH,HSD17B10 | 0.00027 |
| BP | Lipid metabolic process | PEX11A,ACSL4,ACADSB,SOAT1,ABCC3,SCPEP1, ADH1C,ADH5 | 0.0022 |
| BP | Oxidation-reduction process | SUCLG2,ACADSB,PRDX3,SORD,ADH1C,ADH5 | 0.00377 |
| BP | Membrane biogenesis | PEX11A,PEX3 | 0.00473 |
| MF | Transforming growth factor beta receptor, cytoplasmic mediator activity | CDKN1B,SMAD5,SMAD6,SMAD7 | 0.00002 |
| MF | Histone acetyltransferase activity | ING3,GTF3C4,KAT8,TAF1 | 0.00932 |
| MF | Misfolded protein binding | EDEM3,HSPD1 | 0.01072 |
| CC | Protein serine/threonine phosphatase complex | PPM1E,PPP2R5E,PPP3R1,STRN | 0.00828 |
| CC | Peroxisomal membrane | PEX11A,ACSL4,PEX3 | 0.03851 |
| MP | Abnormal kidney morphology | CDKN1B,ADD2,ADM,SGPL1,SLC3A1,HEXB,PPP3 R1 | 0.00624 |
| MP | Abnormal cardiomyocyte apoptosis | ADM,MAPK9,CALCRL,TFAM | 0.011 |
| MP | Increased circulating cholesterol level | CDKN1B,SOAT1,SLC3A1,VLDLR,CPE,APOBEC1, EPM2A | 0.014 |

| | | | |
|---|---|---|---|
| MP | Decreased body weight | CDKN1B,PRDX3,CTSF,ADH1C,CNP,SGPL1,SLC3A1 | 0.026 |

BP: Biologic Process ;MF: Molecular function;CC:Cellular components;MP: Mouse phenotype

Table II: Summary of down regulated placental genes in a Novel Mouse Model of Placental insufficiency.

| **Mouse Gene** | **Gene Name** | **P-value** | **fold-change** |
|---|---|---|---|
| **Actc1** | actin, alpha, cardiac muscle 1 | 0.05 | 0.780857404 |
| **Cmtm5** | CKLF-like MARVEL transmembrane domain containing 5 | 0.0109 | 0.696996137 |
| **Gnb2l1;Snord95;Snord96a** | guanine nucleotide binding protein | 0.0499 | 0.760370346 |
| **Mir23a;Mir27a** | microRNA 23a | 0.0203 | 0.739995106 |
| **Mir341** | microRNA 341 | 0.0492 | 0.753284257 |
| **Mir342** | microRNA 342 | 0.0242 | 0.786782502 |
| **Mirlet7i** | microRNA let7i | 0.0425 | 0.792235791 |
| **Myom1** | myomesin 1 | 0.0388 | 0.768817784 |
| **Ncrna00085;Mir125a;Mir99b** | non-protein coding RNA 85 | 0.0335 | 0.770739243 |
| **Prss43** | protease, serine, 43 | 0.0356 | 0.747644271 |
| **Rian;SNORD113** | RNA imprinted and accumulated in nucleus | 0.0299 | 0.666584156 |
| **Slc5a9** | solute carrier family 5 | 0.0339 | 0.806930129 |
| **Slc7a10** | solute carrier family 7 (cationic amino acid transporter, y+ system), member 10 | 0.05 | 0.825981061 |